



Models of Lift and Drag Coefficients of Stalled and Unstalled Airfoils in Wind Turbines and Wind Tunnels

David A. Spera
Jacobs Technology, Inc., Cleveland, Ohio

An errata was added to this document, July 2012

NASA STI Program . . . in Profile

Since its founding, NASA has been dedicated to the advancement of aeronautics and space science. The NASA Scientific and Technical Information (STI) program plays a key part in helping NASA maintain this important role.

The NASA STI Program operates under the auspices of the Agency Chief Information Officer. It collects, organizes, provides for archiving, and disseminates NASA's STI. The NASA STI program provides access to the NASA Aeronautics and Space Database and its public interface, the NASA Technical Reports Server, thus providing one of the largest collections of aeronautical and space science STI in the world. Results are published in both non-NASA channels and by NASA in the NASA STI Report Series, which includes the following report types:

- **TECHNICAL PUBLICATION.** Reports of completed research or a major significant phase of research that present the results of NASA programs and include extensive data or theoretical analysis. Includes compilations of significant scientific and technical data and information deemed to be of continuing reference value. NASA counterpart of peer-reviewed formal professional papers but has less stringent limitations on manuscript length and extent of graphic presentations.
- **TECHNICAL MEMORANDUM.** Scientific and technical findings that are preliminary or of specialized interest, e.g., quick release reports, working papers, and bibliographies that contain minimal annotation. Does not contain extensive analysis.
- **CONTRACTOR REPORT.** Scientific and technical findings by NASA-sponsored contractors and grantees.

- **CONFERENCE PUBLICATION.** Collected papers from scientific and technical conferences, symposia, seminars, or other meetings sponsored or cosponsored by NASA.
- **SPECIAL PUBLICATION.** Scientific, technical, or historical information from NASA programs, projects, and missions, often concerned with subjects having substantial public interest.
- **TECHNICAL TRANSLATION.** English-language translations of foreign scientific and technical material pertinent to NASA's mission.

Specialized services also include creating custom thesauri, building customized databases, organizing and publishing research results.

For more information about the NASA STI program, see the following:

- Access the NASA STI program home page at <http://www.sti.nasa.gov>
- E-mail your question via the Internet to help@sti.nasa.gov
- Fax your question to the NASA STI Help Desk at 301-621-0134
- Telephone the NASA STI Help Desk at 301-621-0390
- Write to:
NASA Center for AeroSpace Information (CASI)
7115 Standard Drive
Hanover, MD 21076-1320



Models of Lift and Drag Coefficients of Stalled and Unstalled Airfoils in Wind Turbines and Wind Tunnels

*David A. Spera
Jacobs Technology, Inc., Cleveland, Ohio*

Prepared under Contract NNC05CA95C

National Aeronautics and
Space Administration

Glenn Research Center
Cleveland, Ohio 44135

ERRATA

Issued July 2012 for

NASA/CR-2008-215434

Models of Lift and Drag Coefficients of Stalled and Unstalled
Airfoils in Wind Turbines and Wind Tunnels

David A. Spera

October 2008

Pg. 18, Equation (12b) should read as follows:

$$\text{If } \alpha \geq ACD1: \quad CD2 = CD1 \max + (CD2\max - CD1 \max) \sin\left(\frac{\alpha - ACD1}{90.0 - ACD1} \bullet 90.0\right) \quad (12b)$$

Level of Review: This material has been technically reviewed by expert reviewer(s).

Available from

NASA Center for Aerospace Information
7115 Standard Drive
Hanover, MD 21076-1320

National Technical Information Service
5285 Port Royal Road
Springfield, VA 22161

Available electronically at <http://gltrs.grc.nasa.gov>

Models of Lift and Drag Coefficients of Stalled and Unstalled Airfoils in Wind Turbines and Wind Tunnels

David A. Spera
Jacobs Technology, Inc.
Cleveland, Ohio 44135

Introduction

Objective

The mathematical models described in this report were developed to meet the need for equations with which to calculate lift and drag coefficients along the spans of torsionally-stiff rotating airfoils of the type used in wind turbine rotors and wind tunnel fans. These airfoils operate in both the unstalled and stalled aerodynamic regimes, and acceptable models must be able to move seamlessly from one regime to the other. The input parameters in the equations defining these models should also be derivable from a minimum of test data, because often only a limited number of lift and drag data points in just the pre-stall regime are available. Because wind turbine and fan airfoils have finite lengths, model equations must contain explicit adjustments for the effects of aspect ratio (length to chord width) on lift and drag.

Because the torsional stiffness of a wind turbine or fan airfoil about its longitudinal axis is normally high, airfoil moment coefficients are significantly less important than lift and drag coefficients, so moment coefficients are not addressed in this study.

Background

This study has its origins in a federal program to develop large-scale horizontal-axis wind turbines for the generation of electricity, which was conducted from 1973 to 1995 at the NASA Lewis (now NASA Glenn) Research Center under the sponsorship of the U.S. Department of Energy [Spera, 1995]. An important element of this program was the development of computer models with which to predict the power performance of propeller-style rotors, including empirical equations for lift and drag coefficients [Viterna, 1982, for example]. Later, Viterna [1991] modified one of these wind turbine models so that it could be used to analyze the power performance of wind tunnel fans.

In the 1980s and 1990s a family of airfoils was developed specifically for application to wind turbines, under the sponsorship of the National Renewable Energy Laboratory (NREL: previously the Solar Energy Research Institute) [Tangler and Somers, 1985; Tangler, 1987; Somers, 1989]. Many of these new airfoils were designed for *stall-controlled rotors*, in which peak rotor power during high-wind operation is limited by aerodynamic stall of its blades. This has led to increased interest in the post-stall performance of airfoils as a subject of both experimental and analytical research [for example Ostowari and Naik, 1994; Lindenburg, 2001; and Tangler and Kocurek, 2005]. Wind tunnel fans, on the other hand, are designed to operate unstalled at small angles of attack, so aerodynamic behavior at large or negative angles of attack are less significant in fan analysis.

In addition to wind tunnel tests of individual airfoils, bench-mark tests were conducted by NREL researchers on a two-bladed, 10.06-m diameter *UAE* (unsteady aerodynamic experiment) wind turbine in the NASA Ames 80- by 120-ft wind tunnel, well into the post-stall regime [Tangler and Kocurek, 2004; Gerber et al., 2005]. Pre-stall and post-stall power performance of this fixed-pitch rotor with its two NREL S809 airfoils [Somers, 1989] were accurately measured over a range of known, steady wind speeds, providing excellent data for calibrating proposed lift and drag models in both the pre-stall and post-stall regimes.

Approach

An empirical approach is applied in this study, in which the trends of test data are identified for a wide variety of airfoils and for the UAE wind turbine. These trends are then modeled by a set of algebraic equations based on the best fit of the model to available test data and not on aerodynamic theory. The lift and drag properties of infinite- and finite-length circular cylinders and thin plates are also modeled by these same empirical equations.

The development of lift and drag models in this study extends and broadens previously published work in several areas, as follows

1. The test data base is significantly broadened to include a wide range of airfoils, aspect ratios, Reynolds numbers, angles of attack, and the presence or absence of leading-edge trip strips.
2. Lift and drag behavior at high angles of attack in the post-stall regime are not assumed to be the same as the behavior of flat plates as in earlier simplified models. Instead, empirical equations are derived based on the measured behavior of the airfoils themselves.
3. Airfoil thickness is added to aspect ratio and angle of attack as another dependent variable in the model equations.
4. Mean and standard deviations of the proposed model from most of the available airfoil test data are calculated. In this way, the accuracy can be measured of the assumption that the lift and drag properties of all airfoils in the post-stall regime can be represented by a single set of models.
5. Wind turbine rotor power and wind tunnel fan pressure rise are calculated on the basis of model lift and drag coefficients as input to a basic *blade element momentum* (BEM) performance code. Mean and standard deviations from measured power are calculated. This permits quantitative evaluation of the assumption that static airfoil lift and drag data can be applied successfully in BEM performance analyzes of rotating turbine and fan blades.

Aerodynamic Loads on an Airfoil Section

Figure 1 illustrates the components of airspeed and force acting on an airfoil section of a fan blade (fig. 1(a)) and a wind turbine blade (fig. 1(b)) at a radial distance r from the axis of rotation. The view in these schematic diagrams is from the blade hub toward the tip. According to the BEM theory, airloads on a section of an airfoil are proportional to the *dynamic pressure* at only that section. Lift and drag coefficients are proportionality constants that enable the calculation of aerodynamic forces, as follows:

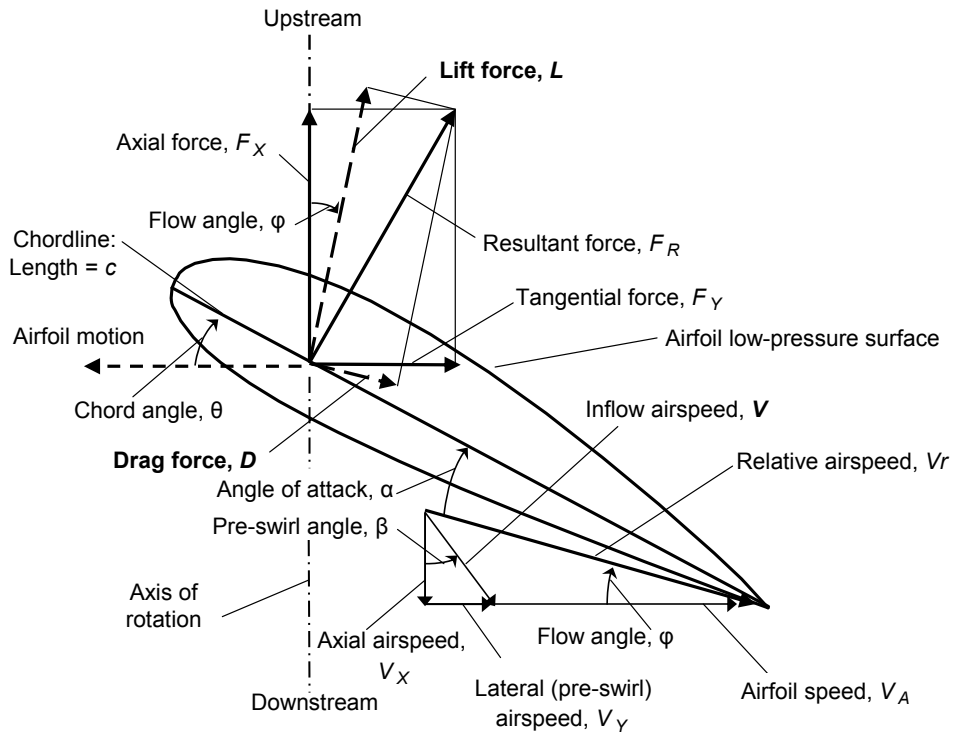
$$L = CL \cdot pd \cdot c \quad (1a)$$

$$D = CD \cdot pd \cdot c \quad (1b)$$

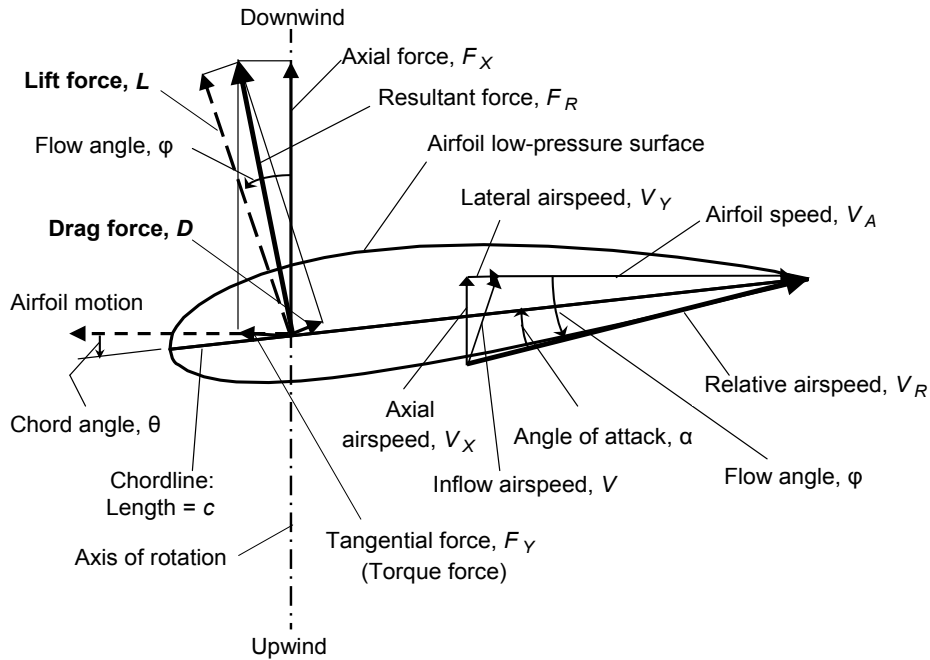
$$pd = 0.5 \rho \cdot Vr^2 \quad (1b)$$

where

L	lift force per unit span; intensity of force perpendicular to relative airspeed (lb/ft)
D	drag force per unit span; intensity of force parallel to relative airspeed (lb/ft)
CL	lift coefficient of the section
CD	drag coefficient of the section
pd	dynamic pressure (lb/ft ²)
ρ	air density (slugs/ft ²)
c	chord length (ft)



(a) Fan blade



(b) Wind turbine blade

Figure 1.—Diagrams of wind and force vectors acting at airfoil sections of fan and wind turbine blades.

Appendix A presents a review of the nomenclature and interaction of wind and force vectors in these figures. Appendix B contains the contours of the NREL S809 and Clark-Y airfoils in the sample applications in this study of the AERODAS lift and drag models.

Airfoil Aspect Ratio

Reference values of aerodynamic coefficients are normally given for infinite-length airfoils, meaning airfoils with no exposed tips that can affect the flow over their span. An airfoil model tested in a wind tunnel may be designed to span from wall to wall or floor to ceiling of the test chamber, to prevent any airflow around the ends of the airfoil and thus to simulate an infinite aspect ratio. Infinite-length airfoil data must be modified before they can be applied to finite-length turbine and fan blades, and this is often done on the basis of the *aspect ratio*, AR , of the blade. An airfoil's aspect ratio is defined as the ratio of its span length to its representative chord width. For a fixed-wing aircraft, airfoil span is equal to the total aerodynamic length of two wings. In the case of a tapered fixed wing, the representative chord is the average chord, so that the aspect ratio of a fixed-wing aircraft is equal to its total aerodynamic planform area divided by the square of its span.

For a finite-length airfoil tested in a wind tunnel, aspect ratio depends on the method of attachment to the airload measuring system in the tunnel floor or wall. In a *reflection plane* test the airfoil is attached without any gap, so its effective span is assumed to be equal to twice its physical span. If there is a gap at the attachment (even a small gap) the high- and low-pressure sides of the airfoil cannot maintain their different pressures. In that case, the airfoil span is taken equal to the physical span of the model.

In this study, the airfoil span of a fan or wind turbine rotor blade is set equal to the total aerodynamically-active length of two blades. For a rotating airfoil, the representative chord is often defined as the chord length at the *mean radius* of the area swept by the blades, which is the radius of a circle that divides the swept area into two equal areas. Thus

$$\pi(Rt^2 - Rm^2) = \pi(Rm^2 - Rh^2) \quad (1a)$$

where

Rt tip radius (ft)
 Rm mean radius (ft)
 Rh hub radius; radius of inner end of active airfoil (ft)

Solving equation (7a) for the mean radius gives

$$Rm = \sqrt{\frac{Rt^2 + Rh^2}{2}} \quad (1b)$$

from which

$$AR = 2(Rt - Rh) / cm \quad (2)$$

where

AR blade aspect ratio based on the mean radius
 cm chord length at mean radius, Rm ; representative chord length (ft)

Lift and Drag Model Configurations

Figures 2(a) and 2(b) illustrate the configurations of the proposed *AERODAS* models for calculating airfoil lift and drag coefficients in both the pre-stall and post-stall regimes, as functions of the angle of attack. As illustrated in figure 1, the angle of attack is the angle from the airfoil chordline to the relative wind vector. Coefficients in the pre-stall and post-stall regimes are modeled separately, and the governing coefficients are selected as follows:

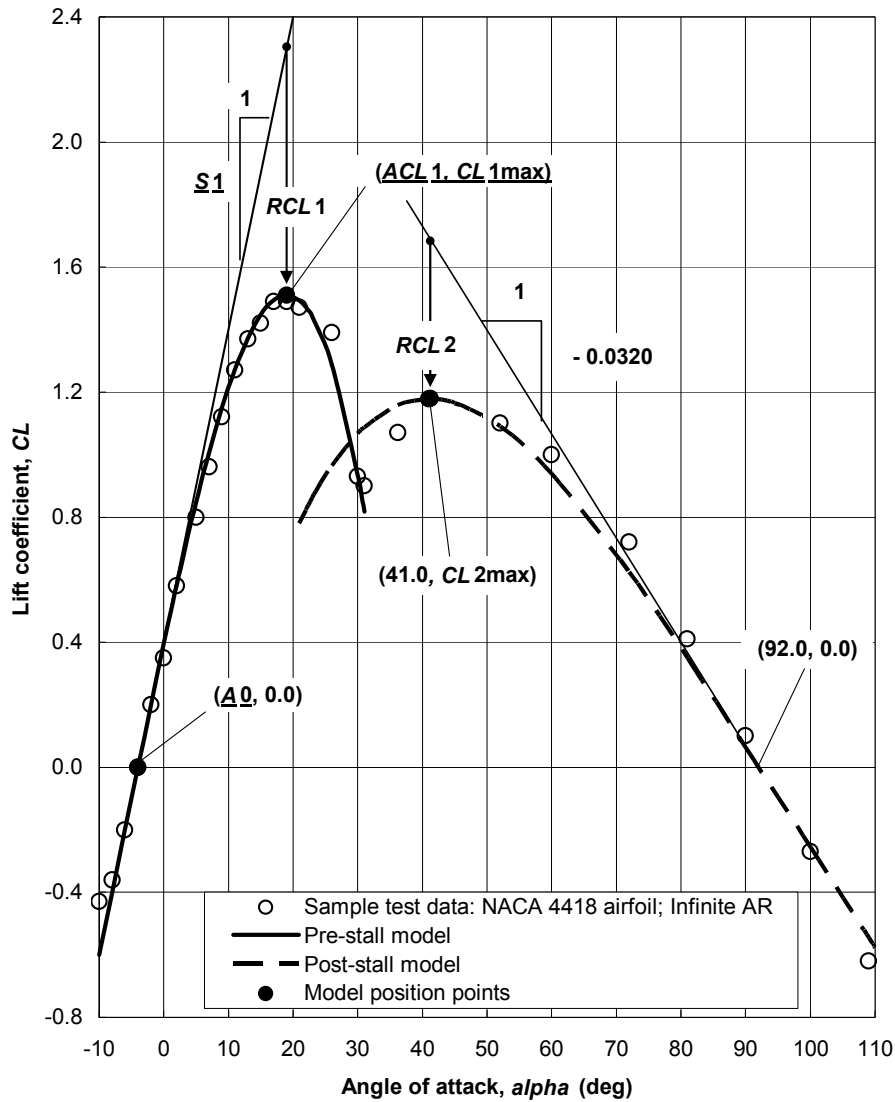
If $\alpha \geq A0$: $CL = \max(CL1, CL2)$ (3a)

If $\alpha < A0$: $CL = \min(CL1, CL2)$ (3b)

$CD = \max(CD1, CD2)$ (3c)

where

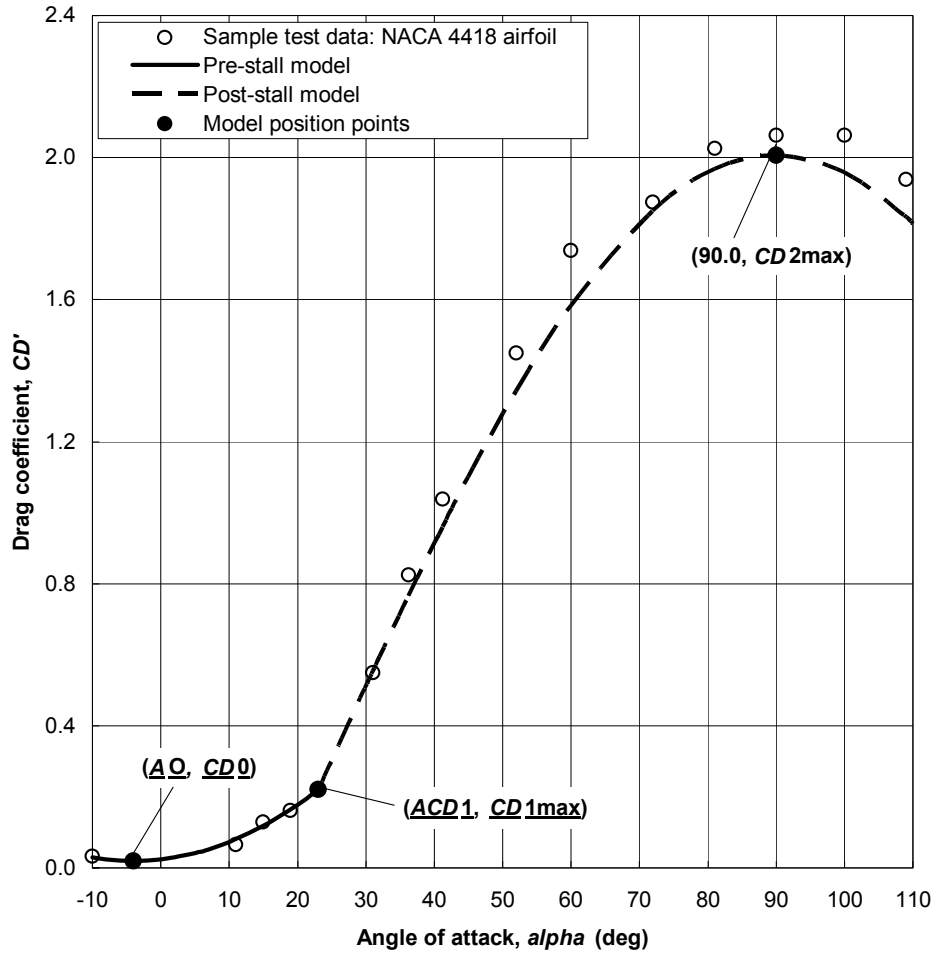
- α angle of attack (deg)
- $A0$ angle of attack at which $CL1 = 0$; for all AR (deg)
- $CL1$ lift coefficient in the pre-stall regime
- $CL2$ lift coefficient in the post-stall regime
- $CD1$ drag coefficient in the pre-stall regime
- $CD2$ drag coefficient in the post-stall regime



(a) Lift coefficient model

Figure 2.—Configurations of the proposed AERODAS models for calculating lift and drag coefficients in the pre-stall and post-stall regimes. Input parameters are underlined.

(a) Lift coefficient model, and (b) drag coefficient model.



(b) Drag coefficient model

Figure 2.—Concluded.

Initial Evaluation of AERODAS Post-Stall Maximum Coefficients

Before detailing the development of the AERODAS lift and drag coefficient equations, an initial evaluation of their accuracy will be made using post-stall test data collected by Lindenburg [2000]. In this reference, maximum post-stall lift and drag coefficients, $CL2max$ and $CD2max$, of 29 varieties of airfoils are presented and compared with coefficients calculated using the Lindenburg StC model. In addition to the airfoil's aspect ratio, the StC model considers the effects of the sizes of the radii of the leading and trailing edges.

For this initial evaluation, post-stall maximum coefficients calculated using the AERODAS model are compared to (a) the Lindenburg data set of measured coefficients, (b) the reported StC model calculations, and (c) flat-plate model calculations, the latter chosen because of the often-used assumption that all airfoils act like flat plates at high angles of attack. Maximum lift and drag coefficients in the flat-plate model are calculated here according to the following empirical curve-fit equations:

$$\alpha = 90^\circ: \quad CD2max = 1.98 [0.60 + 0.40 \exp(-20/AR)] \quad (4a)$$

$$\alpha = 45^\circ: \quad CL2max = 1.17 [0.67 + 0.33 \exp(-20/AR)] \quad (4b)$$

Equation (4a) is a curve-fit of flat-plate drag data from Hoerner [1961] and Binder [1955]. Equation (4b) is a curve fitted to lift data from Hoerner at $1/AR = 0$ and 1.0 , assuming that lift has the same exponential decay rate with respect to aspect ratio as drag (i.e., $-20/AR$).

Tables 1 and 2 are tabulations of the Lindenburg collection of test data compared with calculations by the AERODAS, StC, and flat-plate models. The deviation statistics at the bottom of each of these tables indicate that the AERODAS model predicts maximum post-stall lift and drag coefficients with acceptable accuracy for a wide variety of airfoils and airfoil conditions. The mean and standard deviations between AERODAS calculations and test data are significantly less than those of the other two models. Tables 3 and 4 list the deviations of AERODAS coefficients from measured maximum lift and drag coefficients in the post-stall regime. The largest deviations occur when the StC and flat-plate models are applied to finite-length airfoil data, which is expected to be a significant deficiency for their application in turbine and fan performance analysis.

TABLE 1.—POST-STALL MAXIMUM LIFT COEFFICIENTS CALCULATED ACCORDING TO THREE MODELS AND COMPARED TO MEASURED COEFFICIENTS.
[Test data sources: see Lindenburg 2000]

Airfoil designation	Thickness ratio, t/c	Aspect ratio, AR	Meas. post-stall max lift coef., CL_{2max}	Model calculations of post-stall max lift coef., CL_{2max}		
				AERODAS model	StC model	Flat-plate model
NACA 0012	0.12	Inf.	1.111	1.173	1.143	1.170
NACA 0012	0.12	Inf.	1.118	1.173	1.143	1.170
NACA 0015	0.15	Inf.	0.933	1.163	1.137	1.170
NACA 4409	0.09	Inf.	1.220	1.180	1.182	1.170
NACA 4412	0.12	Inf.	1.210	1.173	1.174	1.170
NACA 4415	0.15	Inf.	1.200	1.163	1.166	1.170
NACA 4418	0.18	Inf.	1.170	1.151	1.157	1.170
NACA 0012	0.12	Inf.	1.171	1.173	1.143	1.170
NACA 23012	0.12	Inf.	1.217	1.173	1.166	1.170
NACA 23017	0.17	Inf.	1.152	1.156	1.149	1.170
FX-84-W-127	0.13	Inf.	1.232	1.171	1.173	1.170
FX-84-W-218	0.22	Inf.	1.152	1.133	1.175	1.170
LS-421 Mod	0.21	Inf.	1.193	1.138	1.205	1.170
NACA 23024	0.24	Inf.	0.990	1.121	1.122	1.170
NACA 63-215	0.15	Inf.	1.094	1.163	1.176	1.170
GA(W)-1	0.17	Inf.	1.094	1.156	1.213	1.170
GA(W)-1 Inverted	0.17	Inf.	1.094	1.156	1.082	1.170
NACA 4409	0.09	12	1.048	1.014	0.876	0.855
NACA 4412	0.12	12	0.991	1.007	0.871	0.855
NACA 4418	0.18	12	1.002	0.989	0.861	0.855
NACA 4409	0.09	9	0.937	0.919	0.839	0.824
NACA 4412	0.12	9	0.886	0.913	0.834	0.824
NACA 4418	0.18	9	0.814	0.897	0.824	0.824
Clark-Y	0.18	8	0.978	0.856	0.812	0.814
NACA 4409	0.09	6	0.835	0.800	0.802	0.796
NACA 4412	0.12	6		0.795	0.802	0.796
NACA 4418	0.18	6		0.780	0.802	0.796
Clark-Y	0.18	6	0.890	0.779	0.766	0.796
Infinite length airfoils						
Mean deviation of model from test data:				0.021	0.021	0.032
Standard deviation:				0.078	0.074	0.086
Finite-length airfoils:						
Mean deviation of model from test data:				-0.023	-0.100	-0.104
Standard deviation:				0.057	0.115	0.124
All airfoils:						
Mean deviation of model from test data:				0.006	-0.021	-0.015
Standard deviation:				0.074	0.091	0.099

TABLE 2.—POST-STALL MAXIMUM DRAG COEFFICIENTS CALCULATED ACCORDING TO THREE MODELS AND COMPARED TO MEASURED COEFFICIENTS.
[Test data sources: see Lindenburg 2000]

Airfoil designation	Thickness ratio, t/c	Aspect ratio, AR	Meas. post-stall max drag coef., $CD2max$	Model calculations of post-stall max drag coef., $CD2max$		
				AERODAS model	StC model	Flat-plate model
NACA 0012	0.12	Inf.	2.090	2.053	1.902	1.980
NACA 0012	0.12	Inf.	2.090	2.053	1.902	1.980
NACA 0015	0.15	Inf.	1.700	2.007	1.878	1.980
NACA 4409	0.09	Inf.	2.100	2.100	1.985	1.980
NACA 4412	0.12	Inf.	2.060	2.053	1.959	1.980
NACA 4415	0.15	Inf.	2.068	2.007	1.933	1.980
NACA 4418	0.18	Inf.	2.060	1.964	1.906	1.980
NACA 0012	0.12	Inf.	2.050	2.053	1.902	1.980
NACA 23012	0.12	Inf.	2.082	2.053	1.948	1.980
NACA 23017	0.17	Inf.	2.078	1.978	1.902	1.980
FX-84-W-127	0.13	Inf.	2.000	2.042	1.964	1.980
FX-84-W-218	0.22	Inf.	2.040	1.911	1.939	1.980
LS-421 Mod	0.21	Inf.	2.020	1.922	2.010	1.980
NACA 23024	0.24	Inf.	1.970	1.881	1.798	1.980
NACA 63-215	0.15	Inf.	1.980	2.007	1.959	1.980
GA(W)-1	0.17	Inf.	1.830	1.978	2.032	1.980
GA(W)-1 Inverted	0.17	Inf.	1.720	1.978	1.794	1.980
NACA 4409	0.09	12	1.750	1.698	1.370	1.322
NACA 4412	0.12	12	1.690	1.659	1.356	1.322
NACA 4418	0.18	12	1.680	1.587	1.327	1.322
NACA 4409	0.09	9	1.590	1.593	1.296	1.256
NACA 4412	0.12	9	1.640	1.557	1.282	1.256
NACA 4418	0.18	9	1.480	1.490	1.254	1.256
Clark-Y	0.18	8	1.470	1.442	1.251	1.235
NACA 4409	0.09	6	1.450	1.430	1.220	1.197
NACA 4412	0.12	6	1.450	1.398	1.206	1.197
NACA 4418	0.18	6	1.320	1.337	1.177	1.197
Clark-Y	0.18	6	1.360	1.333	1.204	1.197
Infinite length airfoils						
Mean deviation of model from test data:				0.006	-0.072	-0.016
Standard deviation:				0.120	0.139	0.123
Finite-length airfoils:						
Mean deviation of model from test data:				-0.032	-0.267	-0.284
Standard deviation:				0.047	0.278	0.299
All airfoils:						
Mean deviation of model from test data:				-0.009	-0.149	-0.121
Standard deviation:				0.098	0.205	0.210

TABLE 3.—DEVIATIONS OF AERODAS MODEL MAXIMUM LIFT COEFFICIENTS
IN THE POST-STALL REGIME FROM MEASURED COEFFICIENTS.

Detailed data are listed in table 1

Airfoil	Thickness ratio <i>t/c</i>	Aspect ratio <i>AR</i>	Deviation from measured max lift coefficient
Clark-Y	18.4%	8	-12.5%
Clark-Y	18.4%	6	-12.5%
FX-84-W-127	12.7%	Inf.	-5.0%
LS-421 Mod	21.0%	Inf.	-4.7%
NACA 4409	9.0%	6	-4.2%
NACA 23012	12.0%	Inf.	-3.6%
NACA 4409	9.0%	12	-3.3%
NACA 4409	9.0%	Inf.	-3.2%
NACA 4412	12.0%	Inf.	-3.1%
NACA 4415	15.0%	Inf.	-3.1%
NACA 4409	9.0%	9	-1.9%
FX-84-W-218	21.8%	Inf.	-1.6%
NACA 4418	18.0%	Inf.	-1.6%
NACA 4418	18.0%	12	-1.3%
NACA 0012	12.0%	Inf.	0.2%
NACA 23017	17.0%	Inf.	0.3%
NACA 4412	12.0%	12	1.7%
NACA 4412	12.0%	9	3.1%
NACA 0012	12.0%	Inf.	4.9%
NACA 0012	12.0%	Inf.	5.6%
GA(W)-1	17.0%	Inf.	5.6%
GA(W)-1 Inverted	17.0%	Inf.	5.6%
NACA 63-215	15.0%	Inf.	6.3%
NACA 4418	18.0%	9	10.2%
NACA 23024	24.0%	Inf.	13.3%
NACA 0015	15.0%	Inf.	24.7%
NACA 4412	12.0%	6	
NACA 4418	18.0%	6	
Mean deviation:			0.8%

TABLE 4.—DEVIATIONS OF AERODAS MODEL MAXIMUM DRAG COEFFICIENTS
IN THE POST-STALL REGIME FROM MEASURED COEFFICIENTS.

Detailed data are listed in table 2.

Airfoil	Thickness ratio <i>t/c</i>	Aspect ratio <i>AR</i>	Deviation from measured max lift coefficient
FX-84-W-218	21.8%	Inf.	-6.3%
NACA 4418	18.0%	12	-5.5%
NACA 4412	12.0%	9	-5.1%
LS-421 Mod	21.0%	Inf.	-4.9%
NACA 23017	17.0%	Inf.	-4.8%
NACA 4418	18.0%	Inf.	-4.7%
NACA 23024	24.0%	Inf.	-4.5%
NACA 4412	12.0%	6	-3.6%
NACA 4409	9.0%	12	-3.0%
NACA 4415	15.0%	Inf.	-2.9%
Clark-Y	18.4%	6	-2.0%
Clark-Y	18.4%	8	-1.9%
NACA 4412	12.0%	12	-1.8%
NACA 0012	12.0%	Inf.	-1.8%
NACA 0012	12.0%	Inf.	-1.8%
NACA 23012	12.0%	Inf.	-1.4%
NACA 4409	9.0%	6	-1.4%
NACA 4412	12.0%	Inf.	-0.4%
NACA 4409	9.0%	Inf.	0.0%
NACA 0012	12.0%	Inf.	0.1%
NACA 4409	9.0%	9	0.2%
NACA 4418	18.0%	9	0.6%
NACA 4418	18.0%	6	1.3%
NACA 63-215	15.0%	Inf.	1.4%
FX-84-W-127	12.7%	Inf.	2.1%
GA(W)-1	17.0%	Inf.	8.1%
GA(W)-1 Inverted	17.0%	Inf.	15.0%
NACA 0015	15.0%	Inf.	18.1%
Mean deviation:			-0.4%

On the basis of this initial evaluation, it is concluded that (1) the post-stall lift and drag coefficients of a wide variety of airfoils can be predicted with acceptable accuracy with a common model fitted to a sufficient range of test data, (2) the accuracy of the AERODAS model is equal to or greater than comparable models for this purpose, and (3) any predictions based on flat-plate behavior can be expected to underestimate both lift and drag at large angles of attack.

Input Parameters and Adjustments for Finite Aspect Ratio

Figures 2(a) and (b) illustrate seven lift and drag parameters of an airfoil that are input into AERODAS. These parameters are underlined in the figures. Designating parameters for an infinite aspect ratio airfoil by prime notation, the input data are defined as follows:

- A0* angle of attack at which $CL1 = 0$; for all aspect ratios (deg)
- ACL1'* angle of attack at maximum pre-stall lift (deg)
- CL1max'* maximum pre-stall lift coefficient; at $\alpha = ACL1'$
- S1'* slope of linear segment of pre-stall lift curve (1/deg)
- CDO* minimum drag coefficient; at $\alpha = A0$; for all aspect ratios

$ACD1'$ angle of attack at maximum pre-stall drag (deg)
 $CD1max'$ maximum pre-stall drag coefficient; at $\alpha = ACD1'$

Angles of attack $ACL1'$ and $ACD1'$ were assumed to be approximately equal in a previous model [Viterna 1982], which is true for some airfoils. However, two separate inputs are provided in AERODAS to accommodate the more-general case in which they are not equal.

Five of the seven input parameters listed above must be adjusted for aspect ratio before they can be used to model the behavior of finite-length airfoils. Jacobs and Anderson [1929] presented a procedure for adjusting pre-stall aerodynamic coefficients measured with a finite-length model to an infinite aspect ratio condition. In this study, the Jacobs and Anderson adjustment procedure is reversed, in order to adjust infinite aspect ratio data for application to a finite-length airfoil.

In the Jacobs and Anderson procedure, measured angles of attack and drag coefficients are adjusted to convert them from a finite- to an infinite-aspect ratio. Reversing this procedure here, the adjustment is as follows:

$$\alpha = \alpha' + 57.3 CL1' \left(\frac{1 + \tau}{\pi AR} \right) = \alpha' + 57.3 CL1' \bullet E[\tau] \quad (4a)$$

$$CD1 = CD1' + CL1' ^2 \bullet \left(\frac{1 + \sigma}{\pi \bullet AR} \right) = CD1' + CL1' ^2 \bullet E[\sigma] \quad (4b)$$

where

$CL1'$ pre-stall lift coefficient for infinite aspect ratio
 α' angle of attack for infinite aspect ratio for a lift coefficient CL' (deg)
 τ empirical reference term for adjusting angle of attack; function of aspect ratio
 $CD1'$ pre-stall drag coefficient for infinite aspect ratio at a lift coefficient $CL1'$
 σ empirical reference term for adjusting drag coefficient; function of aspect ratio
 $E[]$ aspect ratio adjustment function; function of []

Changing from an infinite to a finite aspect ratio causes an increase in both the angle of attack and the drag coefficient for a given lift coefficient. Jacobs and Anderson evaluated the functions τ and σ in equations (4) for selected aspect ratios. Two empirical equations are introduced here that curve-fit these reference functions, as follows:

$$E[\tau] = \frac{1 + \tau}{\pi AR} = 0.318 AR^{-0.90} \quad (4c)$$

$$E[\sigma] = \frac{1 + \sigma}{\pi AR} = 0.280 AR^{-0.90}$$

Combining equations (4a), (4b), and (4c) gives the following aspect ratio adjustment equations for the pre-stall regime:

$$\alpha = \alpha' + 18.2 CL1' \bullet AR^{-0.90}$$

$$CD1 = CD1' + 0.280 CL1' ^2 \bullet AR^{-0.90} \quad (4d)$$

Four of the primed input parameters given above can now be adjusted to a finite aspect ratio by applying equations (4d), as follows:

$$ACL1 = ACL1' + 18.2 CL1max' \bullet AR^{-0.90} \quad (5a)$$

$$S1 = \frac{S1'}{1 + 18.2 S1' \bullet AR^{-0.90}} \quad (5b)$$

$$ACD1 = ACD1' + 18.2 CL1 \max' \bullet AR^{-0.90} \quad (5c)$$

$$CD1 \max = CD1 \max' + 0.280 CL1 \max'^2 \bullet AR^{-0.90} \quad (5d)$$

The fifth input parameter, $CL1 \max'$, is adjusted on the basis of the following empirical equation derived from $CL1 \max$ test data presented by Ostowari and Naik [1984] for NACA 4415 and 4418 airfoils at four Reynolds numbers, with both tripped and clean leading edges:

$$CL1 \max = CL1 \max' \left\{ 0.67 + 0.33 \exp \left[- (4.0 / AR)^2 \right] \right\} \quad (5e)$$

Equations for Coefficients in the Pre-Stall Regime

Following the method proposed by Viterna [1982 and 1991], the pre-stall lift curve is calculated using the following equations:

$$\text{If } \alpha \geq A0: \quad CL1 = S1 \bullet (\alpha - A0) - RCL1 \left(\frac{\alpha - A0}{ACL1 - A0} \right)^{N1} \quad (6a)$$

$$\text{If } \alpha < A0: \quad CL1 = S1 \bullet (\alpha - A0) + RCL1 \left(\frac{A0 - \alpha}{ACL1 - A0} \right)^{N1} \quad (6b)$$

$$RCL1 = S1 \bullet (ACL1 - A0) - CL1 \max \quad (6c)$$

$$N1 = 1 + CL1 \max / RCL1 \quad (6d)$$

where

$RCL1$ reduction from extension of linear segment of lift curve to $CL1 \max$

$N1$ exponent defining shape of lift curve at $ACL1 \max$

In the absence of test data at negative angles of attack of sufficient magnitude to produce stall, the assumption inherent in Equation (6b) is that the lift curve is anti-symmetric about $\alpha = A0$.

The pre-stall drag curve is commonly defined as a quadratic equation, $M=2.0$, in terms of the angle of attack, as follows:

$$\text{If } (2 A0 - ACD1) \leq \alpha \leq ACD1: \quad CD1 = CD0 + (CD1 \max - CD0) \left(\frac{\alpha - A0}{ACD1 - A0} \right)^M \quad (7a)$$

An exponent M larger than 2.0 is appropriate for some airfoils. This is best determined by fitting equation (7a) to test data in a graph of the airfoil lift-to-drag ratio, $CL1/CD1$, versus angle of attack and then adjusting the exponent for a best fit to the usual valley at small angles of attack.

To facilitate selection of CD in Equation (3c), the following equation is applied:

$$\text{If } \alpha < (2 A0 - ACD1) \text{ or } \alpha > ACD1: \quad CD1 = 0 \quad (7b)$$

Equations for Coefficients in the Post-Stall Regime

Post-Stall Maximum Lift and Drag

Referring again to figure 2, the maximum lift and drag coefficients in the post-stall regime are assumed to be functions of the airfoil's thickness-to-chord ratio and its aspect ratio, arranged in the following form:

$$\text{Figure 2(a): At } \alpha = 41^\circ: \quad CL2 \max = F1[t/c] \bullet F2[AR] \quad (8a)$$

$$\text{Figure 2(b): At } \alpha = 90^\circ: \quad CD2 \max = G1[t/c] \bullet G2[AR] \quad (8b)$$

where

t	airfoil thickness (ft)
$F1, G1$	empirical functions of t/c
$F2, G2$	empirical functions of AR

These empirical functions were selected to give the best fit of AERODAS calculations to two different types of test data: (1) Airfoil test data from several sources [Lindenburg, 2000; Ostowari and Naik, 1984; Tangler and Ostowari, 1995; Hoerner, 1965; and Critzos et al., 1955], and (2) power performance of the full-scale UAE wind turbine tested in a wind tunnel, as reported by Tangler and Kocurek [2004] and Gerber et al., [2005].

Maximum Lift

The empirical equations developed for calculating maximum post-stall lift coefficients are as follows:

$$F1 = 1.190 [1.0 - (t/c)^2] \quad (9a)$$

$$F2 = 0.65 + 0.35 \exp [-(9.0/AR)^{2.3}] \quad (9b)$$

Figure 3 illustrates the application of equations (9), in which calculations of $CL2\max$ can be compared with test data for ranges of thickness and aspect ratio. Airfoil thicknesses are typically less than 25 percent of chord, so thickness in this range is seen to have only a minor effect on lift. However, equation (9b) adequately defines the overall trend between thin plates with t/c equal to zero and round cylinders with t/c of unity.

The NREL S809 airfoils in the UAE wind turbine rotor have a thickness ratio of 21 percent and an aspect ratio of 15.3, calculated in accordance with equation (2). The trend curve and data point representing the post-stall maximum lift of the UAE turbine blades are noted in figure 3.

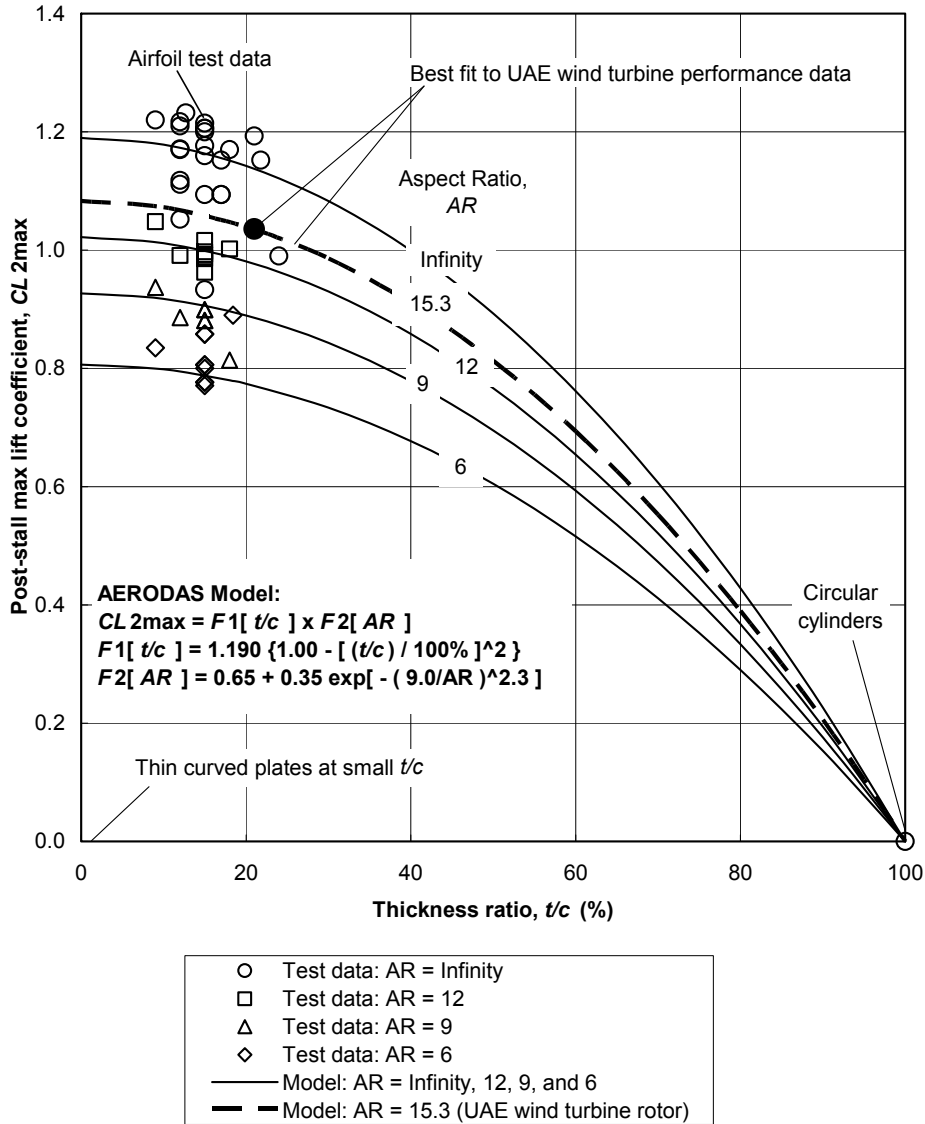


Figure 3.—AERODAS models of post-stall maximum lift coefficients for various airfoil thicknesses and aspect ratios, compared with test data.

Maximum Drag

The empirical equations developed for calculating maximum post-stall drag coefficients are as follows:

$$G1 = 2.300 \exp\{-[0.65(t/c)]^{0.90}\} \tag{10b}$$

$$G2 = 0.52 + 0.48 \exp[-(6.5/AR)^{1.1}] \tag{10c}$$

Figure 4 illustrates the application of equations (10). Again, calculations of CD_{2max} can be compared with test data for ranges of thickness and aspect ratio. Airfoil thickness appears to have more of an effect on drag than on lift. In addition to airfoil data, equation (10b) was developed to fit curved plate,

oval, and circular cylinder drag data [Hoerner, 1961]. The trend curve and data point representing the post-stall maximum drag of the UAE turbine blades are noted in figure 4.

Variation of Post-Stall Lift with Angle of Attack

Referring again to figure 2(a), lift variation with angle of attack in the post-stall regime is modeled in AERODAS by an equation of the same form as that applied in the pre-stall regime, but with a reversed slope, as follows:

$$\text{If } 0 < \alpha < ACL1: \quad CL2 = 0 \quad (11a)$$

$$\text{If } ACL1 \leq \alpha \leq 92.0^\circ: \quad CL2 = -0.032(\alpha - 92.0) - RCL2 \bullet \left(\frac{92.0 - \alpha}{51.0} \right)^{N2} \quad (11b)$$

$$\text{If } \alpha > 92.0^\circ: \quad CL2 = -0.032(\alpha - 92.0) + RCL2 \bullet \left(\frac{\alpha - 92.0}{51.0} \right)^{N2} \quad (11c)$$

$$RCL2 = -0.032(41.0 - 92.0) - CL2_{\max} = 1.632 - CL2_{\max} \quad (11d)$$

$$N2 = 1 + CL2_{\max} / RCL2 \quad (11e)$$

where

$RCL2$ reduction from extension of linear segment of lift curve to $CL2_{\max}$

$N2$ exponent defining shape of lift curve at $CL2_{\max}$

Post-stall lift behavior at a negative angle of attack is assumed to be anti-symmetric about $\alpha = A0$, so that

$$\text{If } \alpha < 0^\circ: \quad CL2[\alpha] = -CL2[-\alpha + 2A0] \quad (11f)$$

Figure 5(a) shows a typical family of post-stall lift curves, in which model calculations are compared with lift coefficient test data for NACA 4415 airfoils with and without leading-edge trip strips. These wind tunnel tests were conducted at a Reynolds number of 250,000 [Ostowari and Naik, 1984].

Trigonometric functions have been used previously for the variation of post-stall lift coefficients with angle of attack, but the power-law configuration in equations (11) was found to be more representative of test data for the finite-length airfoils in this study. As observed by Ostowari and Naik, decreasing aspect ratio flattens the peak of the post-stall lift curve. This behavior is modeled by equations (11) but not by trigonometric functions. Deviations from the model to 231 post-stall lift test data points for NACA 0012, 4415, and 4418 airfoils are as follows:

Mean deviation: 0.012

Standard deviation: 0.038

The data set includes Reynolds numbers from 250,000 to 1,200,000 and leading-edge trip strips.

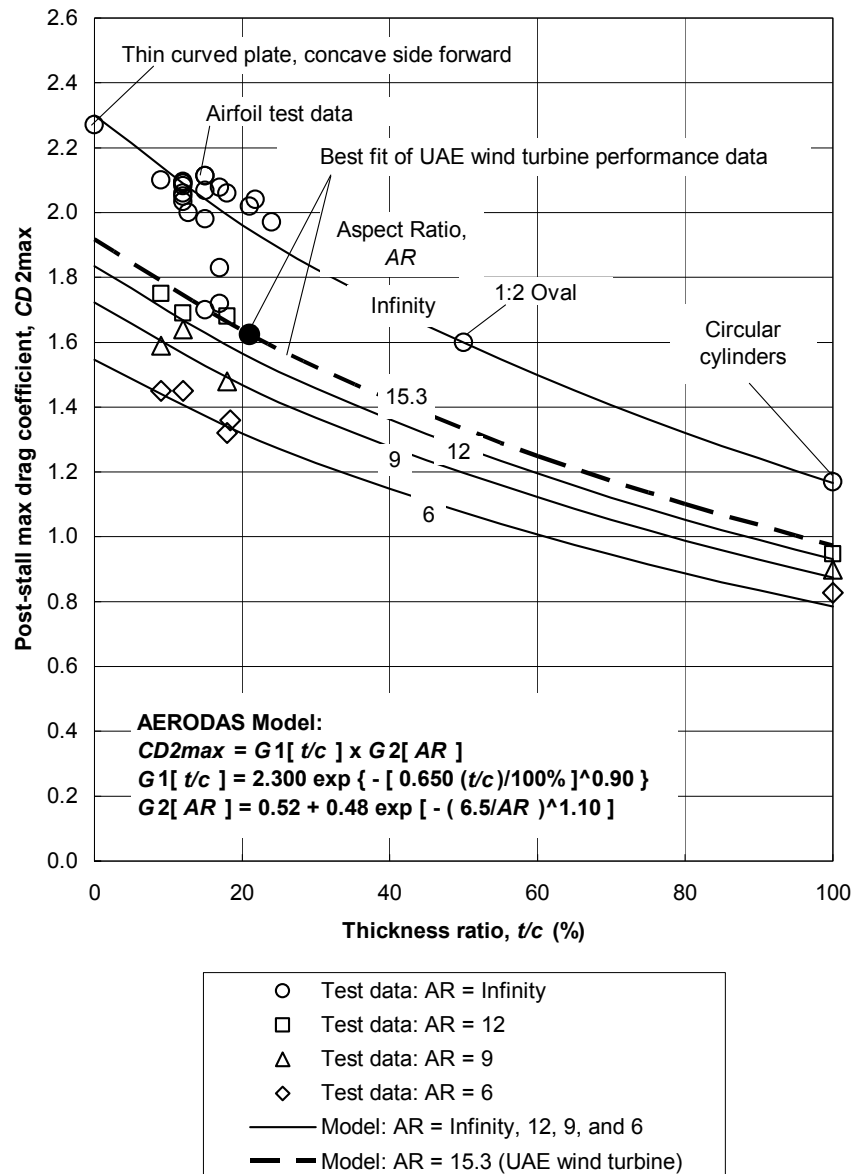
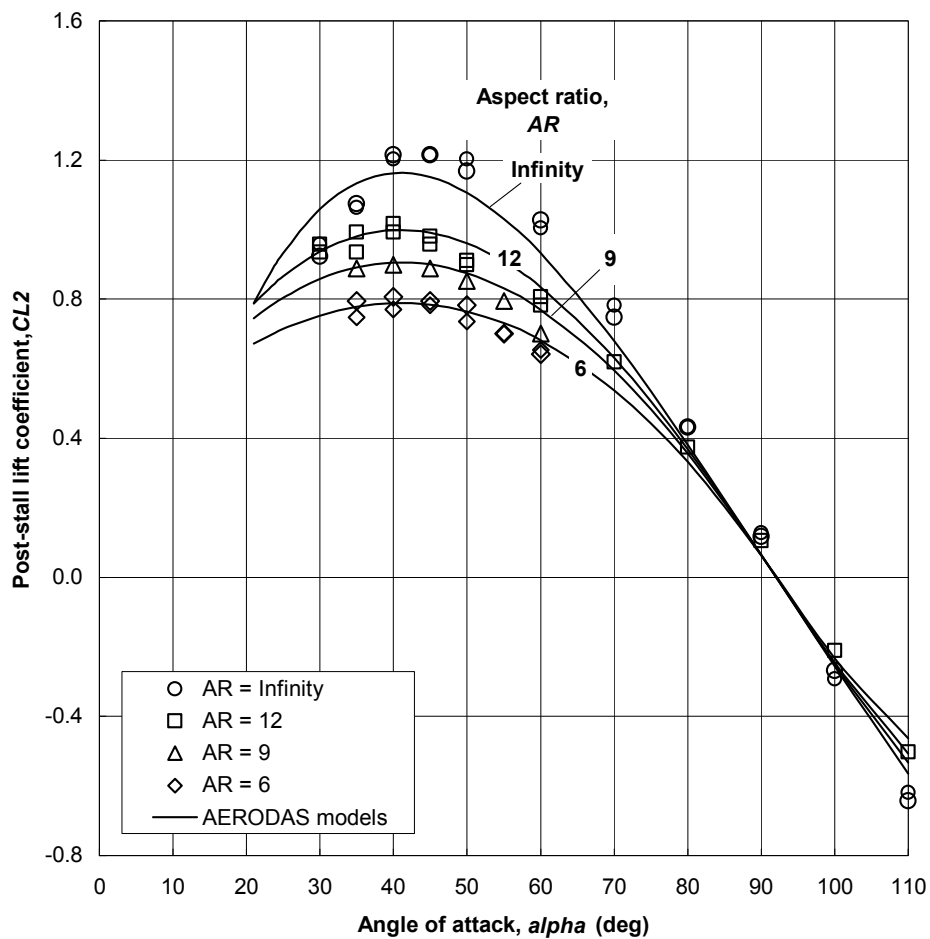


Figure 4. —AERODAS models of post-stall maximum drag coefficients for various airfoil thicknesses and aspect ratios, compared with test data.



(a) Post-stall lift coefficients

Figure 5.—AERODAS models of post-stall lift and drag curves for several aspect ratios compared with test data for NACA 4415 airfoils with and without leading-edge trip strips. Reynolds number = 250,000 [data from Ostowari and Naik, 1984]. (a) Post-stall lift coefficients. (b) Post-stall drag coefficients.

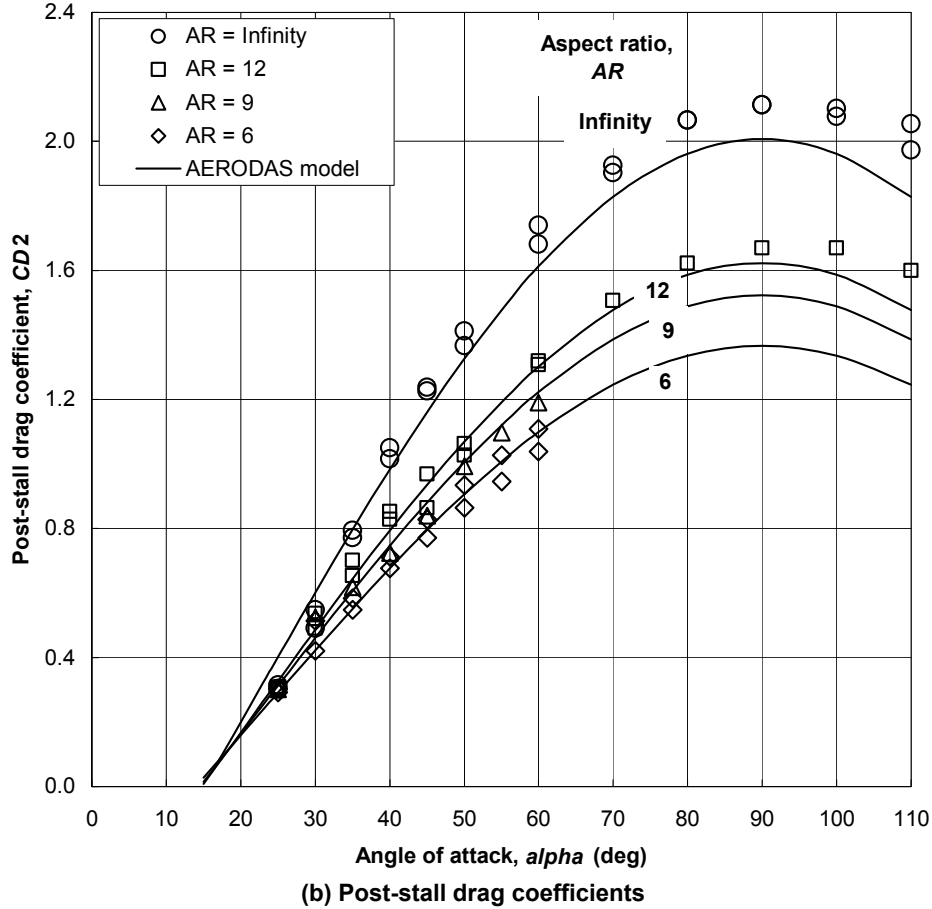


Figure 5.—Concluded.

Variation of Post-Stall Drag with Angle of Attack

Referring to figure 2(b), the drag variation with angle of attack in the post-stall regime is modeled in AERODAS by a sine curve that peaks at an angle of attack of 90° and intersects the pre-stall drag curve at coordinates $(ACD1, CD1max)$, as follows:

$$\text{If } (2A0 - ACL1) < \alpha < ACL1: \quad CD2 = 0 \quad (12a)$$

$$\text{If } \alpha \geq ACD1: \quad CD2 = CD1max + (CD2max - CD1max) \sin\left(\frac{\alpha - ACD1}{90.0 - ACD1} \bullet 90.0\right) \quad (12b)$$

At negative angles of attack, the post-stall drag model is symmetrical about $\alpha = A0$, as follows:

$$\text{If } \alpha \leq (2A0 - ACD1): \quad CD2[\alpha] = CD2[-\alpha + 2A0] \quad (12c)$$

Figure 5(b) shows a family of post-stall drag curves compared with NACA 4415 airfoil test data. In this case, the input parameters $ACD1'$ and $CD1max'$ are 20.0° and 0.200 .

Deviations from the model to 263 post-stall drag test data points for NACA 0012, 4415, and 4418 airfoils are as follows:

Mean deviation: -0.016
Standard deviation: 0.044

The data set includes Reynolds numbers from 250,000 to 1,200,000, some with leading-edge trip strips and upwind trailing edges.

Application of AERODAS Models to Calculation of Wind Turbine Power

The UAE wind turbine has a two-bladed rotor with a tip radius of 16.5 ft, hub radius of 4.13 ft, a tip chord of 1.17 ft, and a hub chord of 2.42 ft. In accordance with equations (1) and (2), the aspect ratio for the NREL S809 rotor blades is 15.3. From the coordinates listed in appendix B, their thickness ratio is 21 percent.

In these wind tunnel tests [Tangler and Kocurek, 2004], the rotor speed was controlled to a relatively low 72 rpm at wind speeds up to 56 mph. This low speed placed much of the blade aerodynamic operation in the post-stall regime. Angles of attack reached almost 50°. As a result, the calculated UAE rotor power is very sensitive to the model parameters, so these UAE performance data points are an excellent guide to parameter selection.

The AERODAS model input data for the S809 airfoils, based on pre-stall lift and drag data [TU Delft, as reported by Lindenburg 2003 and Tangler and Kocurek 2005], are listed in table 5. Figure 6 shows the measured lift and drag test coefficients for an aspect ratio of infinity compared with AERODAS coefficient models for aspect ratios of infinity and 15.3, the aspect ratio of the UAE wind turbine rotor.

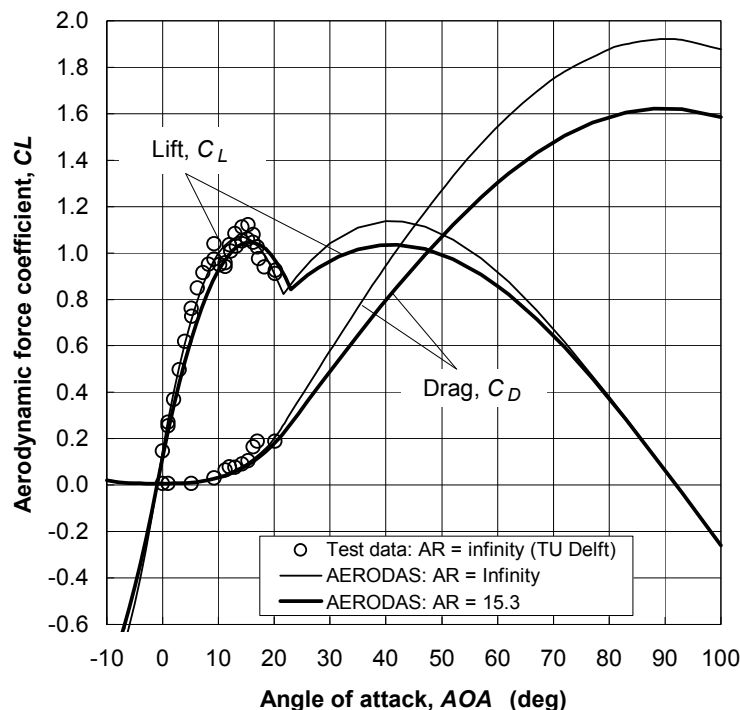


Figure 6.—Measured and calculated lift and drag coefficients for NREL S809 airfoils with the UAE blade aspect ratio of 15.3, compared with reference coefficients for an infinite aspect ratio.

TABLE 5.—AERODAS LIFT AND DRAG MODEL
PARAMETERS FOR NREL SERI S809 AIRFOILS

Constants for All Airfoils			
<i>ACL2</i>		41.0	
<i>ACL3</i>		92.0	
<i>S2</i>		-0.0320	
<i>ACD2</i>		90.0	
Constants for Specific Airfoil			
Name		S809 Smooth	
<i>AR</i>		10,000	
<i>t/c</i>		21	
<i>A0</i>		-1.00	
<i>ACL1'</i>		14.0	
<i>ACD1'</i>		20.1	
<i>S1'</i>		0.155	
<i>CL1max'</i>		1.070	
<i>CD0</i>		0.0070	
<i>CD1max'</i>		0.2000	
<i>M</i>		3.0	
<i>F1</i>		1.138	
<i>G1</i>		1.922	
Lift/Drag Model Parameters			
	Reference	Test Data	Blade
<i>AR</i>	10,000.00	10,000.00	15.28
<i>1/AR</i>	0.0001	0.0001	0.0654
<i>S1</i>	0.155	0.155	0.125
<i>ACL1</i>	14.0	14.0	15.7
<i>ACD1</i>	20.1	20.1	21.8
<i>CL1max</i>	1.070	1.070	1.047
<i>RCL1</i>	1.254	1.254	1.033
<i>N1</i>	1.85	1.85	2.01
<i>CD1max</i>	0.200	0.200	0.226
<i>CL2max</i>	1.138	1.138	1.036
<i>RCL2</i>	0.494	0.494	0.596
<i>N2</i>	3.30	3.30	2.74
<i>CD2max</i>	1.921	1.921	1.624

Figure 7 illustrates the results of calculating rotor power output using lift and drag coefficients from the AERODAS model in a proprietary BEM model of the rotor. Calculated power curves closely match the test behavior with stall-controlled peaks at wind speeds of 10 to 12 m/s and valleys at 16 to 17 m/s.

Deviations of the calculated power points from the 54 test points are as follows:

Mean deviation -0.1 kW = -1.3 percent
Standard deviation 0.4 kW = 4 percent

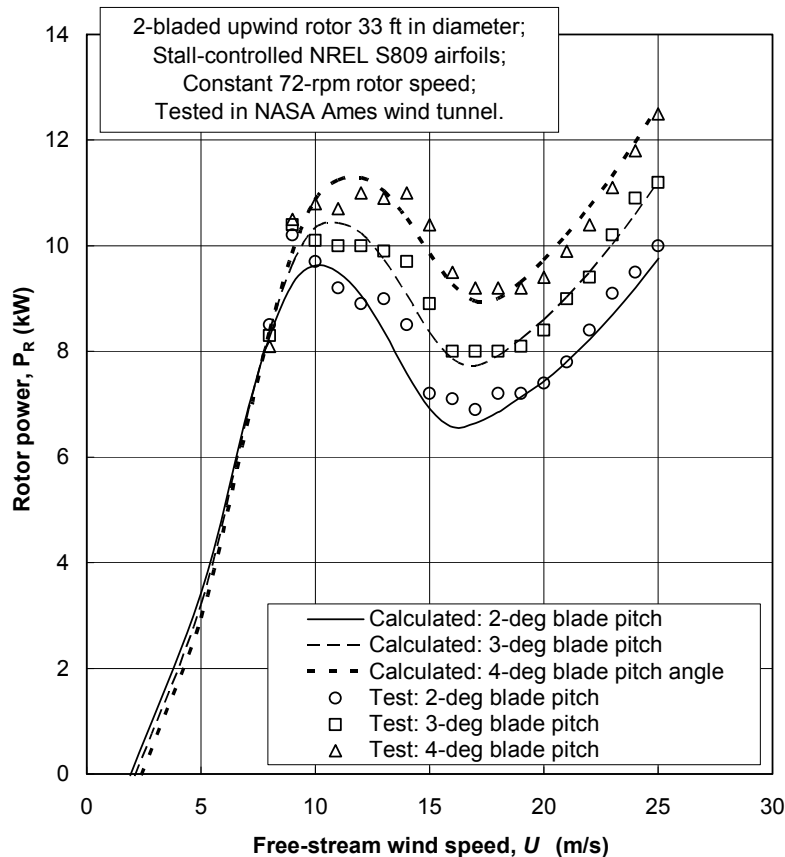


Figure 7.—Calculated rotor power curves of the NREL UAE wind turbine compared with power measured in wind tunnel tests. Calculations are based on AERODAS models of lift and drag coefficients [turbine data reference: Tangler and Kocurek, 2004].

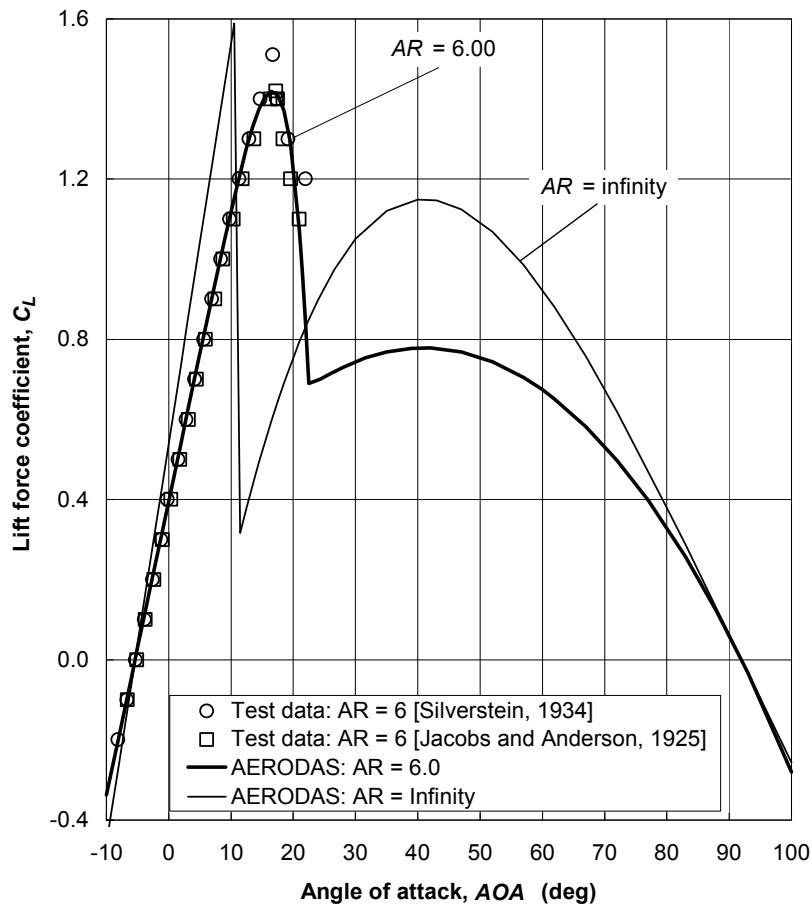
Application of AERODAS Models to Calculating Wind Tunnel Fan Performance

The Icing Research Tunnel (IRT) located at the NASA Glenn Research Center in Cleveland, Ohio, is a closed-loop facility powered by a twelve-bladed fan with a tip radius of 12.57 ft and a hub radius of 5.01 ft, driven by a 5,000-hp electric motor [Irvine *et al* 2001]. The test section of the IRT is 9-ft wide and 6-ft high, in which airspeeds can reach 400 mph. Fan blade sections are Clark-Y airfoils with tip chords of 1.50 ft and hub chords of 2.25 ft. The aspect ratio of the fan blades is 9.04. Referring to the coordinates listed in appendix B, their thickness ratio is 18.4 percent.

Reference lift and drag coefficients [Jacobs and Anderson 1925, Silverstein 1934] were measured using wind tunnel test models with aspect ratios of 6.0. Figure 8 shows these test data curve-fitted with AERODAS models. Infinite aspect ratio parameters were adjusted to best fit the test data at their measured aspect ratio of 6.0. Figure 9 shows the AERODAS lift and drag coefficients for the IRT fan blade aspect ratio of 9.04. Parameters for aspect ratios of infinity (reference), 6.0 (test data), and 9.04 (fan blades) are listed in table 6.

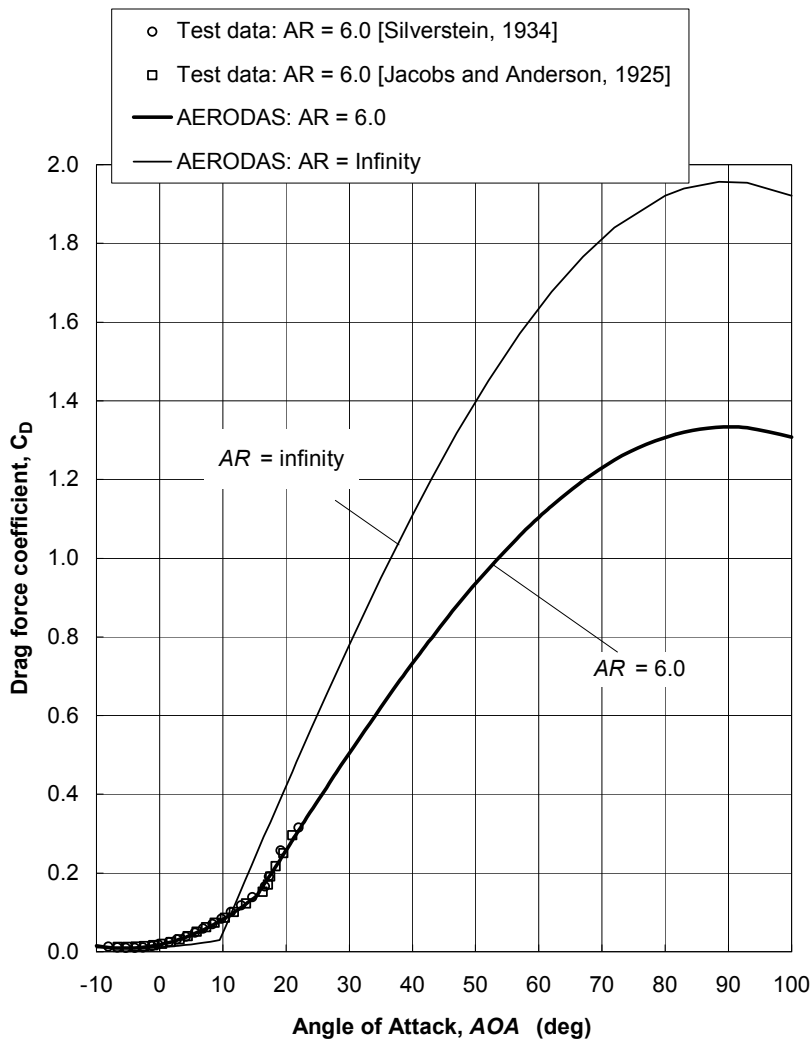
TABLE 6.—AERODAS LIFT AND DRAG MODEL
PARAMETERS FOR CLARK-Y AIRFOILS

Constants for All Airfoils			
<i>ACL2</i>		41.0	
<i>ACL3</i>		92.0	
<i>S2</i>		-0.0320	
<i>ACD2</i>		90.0	
Constants for Specific Airfoil			
Name		Clark Y	
<i>AR</i>		10,000	
<i>t/c</i>		18.4	
<i>A0</i>		-5.40	
<i>ACL1'</i>		10.8	
<i>ACD1'</i>		9.5	
<i>S1'</i>		0.1000	
<i>CL1max'</i>		1.610	
<i>CD0</i>		0.0086	
<i>CD1max'</i>		0.0290	
<i>M</i>		2.0	
<i>F1</i>		1.150	
<i>G1</i>		1.958	
Lift/Drag Model Parameters			
	Reference	Test Data	Blades
<i>AR</i>	10,000.00	6.00	9.04
<i>1/AR</i>	0.0001	0.1667	0.1106
<i>S1</i>	0.1000	0.0734	0.0799
<i>ACL1</i>	10.8	16.6	14.8
<i>ACD1</i>	9.5	15.3	13.5
<i>CL1max</i>	1.610	1.419	1.515
<i>RCL1</i>	0.010	0.198	0.103
<i>N1</i>	162.07	8.17	15.78
<i>CD1max</i>	0.029	0.141	0.118
<i>CL2max</i>	1.150	0.779	0.897
<i>RCL2</i>	0.482	0.853	0.735
<i>N2</i>	3.38	1.91	2.22
<i>CD2max</i>	1.958	1.333	1.487



(a) Lift coefficients

Figure 8.— Measured and calculated aerodynamic lift and drag coefficients for Clark-Y airfoils. Coefficients for an infinite aspect ratio are determined by the best fit of calculated coefficients for an aspect ratio of 6.0.



(b) Drag coefficients

Figure 8.—Concluded.

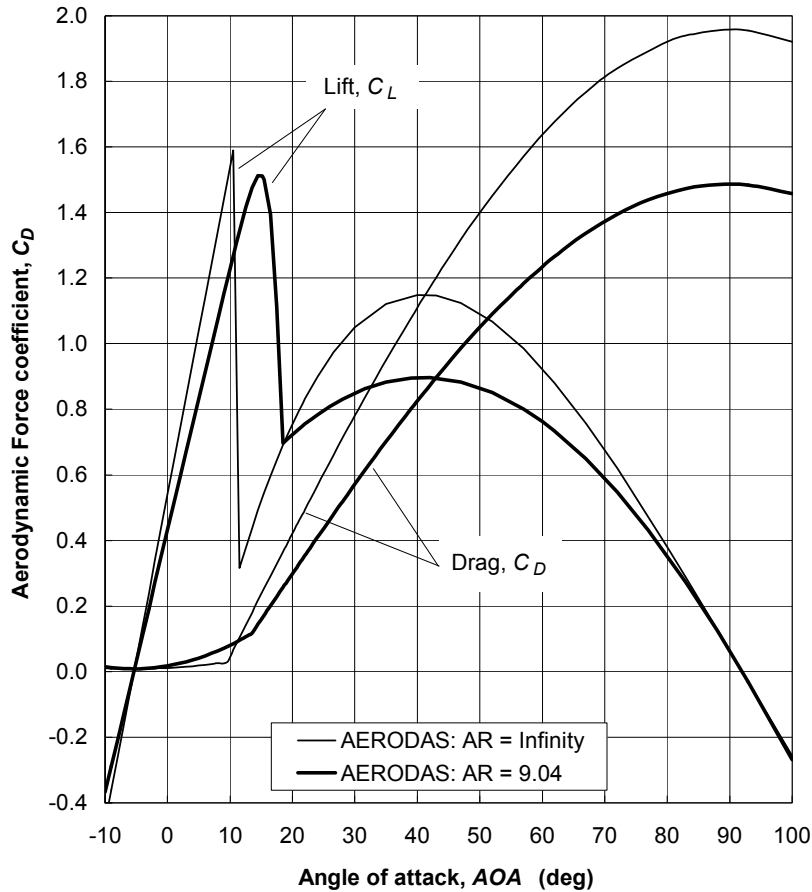


Figure 9.—Calculated lift and drag coefficients for Clark-Y airfoils at the IRT blade aspect ratio of 9.04, compared with reference coefficients for an infinite aspect ratio.

Figure 10 shows the results of calculating the pressure rise across the IRT fan as a function of the wind speed in the tunnel test section, with comparison to test data [Sheldon *et al* 1996]. The lower curve in this figure is the calculated pressure rise with an empty test section, which is the lowest drag condition of the tunnel. The upper curve is the calculated pressure rise for operations with model blockage in the test section and additional drag from ice on the model and surfaces throughout the tunnel loop, with the fan is operating at its maximum speed of 449 rpm. The area between these two curves is the operating regime of the IRT fan. Deviations of the calculated pressure rises from the 22 test points are as follows:

Mean deviation	1.0 psf = 2.7 percent
Standard deviation	1.6 psf = 4.4 percent

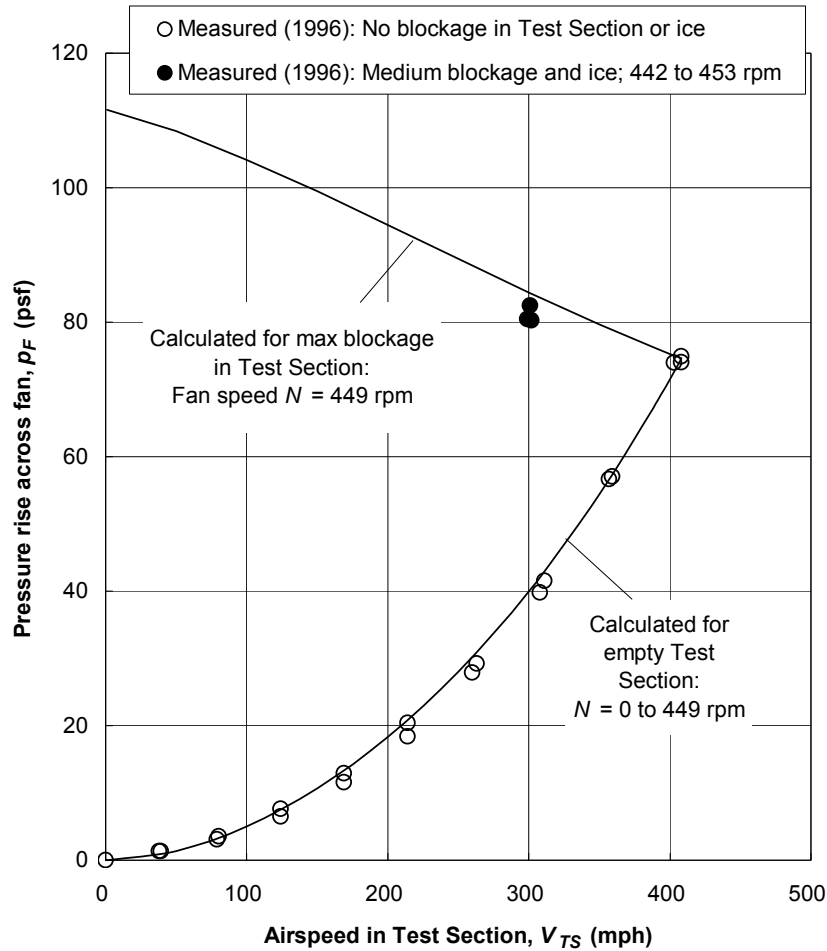


Figure 10.—Calculated fan pressure rises across the NASA Glenn IRT wind tunnel fan compared with measured pressure rises. Calculations are based on AERODAS models of lift and drag coefficients for the fan blades' Clark-Y airfoils.

Summary of Model Deviations

A principal objective of this study was a quantitative assessment of the accuracy of a common model for lift and drag coefficients, evaluated against a wide variety of test data. Table 7 lists the results of this assessment. Model calculations closely fit the average of the 585 lift and drag coefficients of various static airfoils and elements, with a mean deviation of -0.004 and a standard deviation of 0.048 . With respect to the operating wind turbine tests, power calculations based on AERODAS lift and drag coefficients fit measured power with a mean deviation of -1.3 percent and a standard deviation of 4.0 percent. When calculating the pressure rise across a large wind tunnel fan, mean and standard deviations were found to be 2.6 and 4.4 percent, respectively, when AERODAS lift and drag models were used.

TABLE 7.—SUMMARY OF DEVIATIONS BETWEEN AERODAS MODEL CALCULATIONS AND TEST DATA

Type of test	Aspect ratio range	Type of data	Number of data points	Mean deviation	Standard deviation
Airfoils; circular cylinders; oval, curved, and square plates	∞ to 6.0	Max post-stall lift coef.	52	-0.015	0.059
		Max post-stall drag coef.	39	-0.045	0.088
Airfoils with and without LE trip strips	∞ to 6.0	Post-stall lift coef. versus angle of attack	231	0.020	0.038
		Post-stall drag coef. versus angle of attack	263	-0.017	0.045
Total of all elements above	∞ to 6.0	Post-stall lift and drag coefficients	585	-0.004	0.048
UAE wind turbine: NREL S809 airfoils; 3 pitch angles; Stall control of power	15.3	Rotor power versus free-stream wind speed	54	-1.3%	4.0%
IRT wind tunnel fan: Clark-Y airfoils; With and without model in test section and ice	9.04	Pressure rise across fan versus airspeed in test section	22	2.7%	4.4%

Concluding Remarks

This report documents the derivation of equations contained in the AERODAS model, which provides a convenient method for calculating pre-stall and post-stall lift and drag characteristics of rotating airfoils of the type used in wind tunnel fans and wind turbine rotors. The basic parameters in the model can be obtained by fitting simple curves to a limited amount of pre-stall wind tunnel test data. The post-stall models, which are the same for all airfoils, include the effects of airfoil thickness as well as aspect ratio. To date, model calculations of lift and drag coefficients are in close agreement with a large quantity of reference test data for a wide variety of airfoils. Calculations of wind turbine power and fan pressure rise based on AERODAS lift and drag coefficients are also in close agreement with test data.

Appendix A—Aerodynamic Loads on an Airfoil Section

The commonly-used *blade element momentum* (BEM) model of airloads on a section of a fan or turbine blade was used in this study to guide the selection of parameters in the proposed AERODAS lift and drag models. The BEM model is so-called because the aerodynamic forces acting on each cross-section or element of the blade are assumed to be independent of all other elements. Figure 1 illustrates the components of airspeed and force acting on an airfoil section of a fan blade (fig. 1(a)) and a wind turbine blade (fig. 1(b)) at a radial distance r from the axis of rotation. The view in these schematic diagrams is from the blade hub toward the tip. The airfoil sections are moving from right to left at a tangential speed given by

$$Va = r\Omega = \pi r N / 30 \quad (\text{A1})$$

where

Va	airfoil section tangential speed (ft/s)
r	radial coordinate of airfoil section (ft)
Ω	shaft rotational speed (rad/s)
N	shaft rotational speed (rpm)
π	3.1416

The *chordline* of the airfoil section and its direction of motion form an angle θ which is referred to here as the *chord angle* and which typically varies with the radial coordinate r . The chord angle is equal to the sum of the local built-in *twist angle*, γ , and the adjustable *blade pitch angle*, δ . The blade pitch angle is constant for all sections of the blade.

As shown in figure 1, the speed of the airflow acting on the section is resolved into axial and lateral components, Vx and Vy , respectively. These airspeed components may have a non-uniform radial distribution from the axis of rotation outward to the blade tip. In the airflow model of the UAE wind turbine used in this study, radial airspeed distributions are assumed to be constant and axisymmetric. Airfoil loads caused by asymmetric airflow, such as wind shear across a wind turbine rotor or non-uniform inflow to a wind tunnel fan, can be calculated at selected blade azimuthal positions and then integrated for one complete rotation of the rotor. This process is referred to as a *quasi-static analysis* and is useful for obtaining a first-order approximation to the dynamic airloads caused by a non-uniform inflow.

In a wind tunnel fan, figure 1(a), an axisymmetric lateral or *pre-swirl* inflow component may be induced by an array of stationary radial vanes (inlet guide vanes) directly upstream. Pre-swirl is directed to oppose the airfoil motion for two purposes: (1) To increase the pressure rise across the fan for a given fan shaft speed, and (2) to offset swirl in the fan wake that is subsequently induced by the blades in the same direction as their motion. Reducing swirl in the wake tends to reduce aerodynamic losses at the fan.

The *relative airspeed* acting on the airfoil at a *flow angle* ϕ to the direction of its motion is defined by the vector addition of the airflow speed components and the airfoil tangential speed, as follows:

$$Vr = \sqrt{Vx^2 + (Va + Vy)^2} \quad |$$

$$Vx = Vxt \bullet [1 + a(1 - r/Rt) + b(1 - r/Rt)^2]$$

$$Vy = Vx \tan(\beta) \quad (\text{A2})$$

$$\phi = \arctan[Vx/(Va + Vy)]$$

where

Vr	relative airspeed (ft/s)
Vx	axial component of airspeed (ft/s)

V_y	pre-swirl (lateral) component of airspeed (ft/s)
V_{xt}	axial component of airspeed at blade tip radius (ft/s)
a, b	empirical constants defining the radial distribution of the axial airspeed
R_t	blade tip radius (ft)
β	pre-swirl angle; angle from the axis of rotation to the inflow airspeed vector (deg)
φ	flow angle; angle from the direction of airfoil motion to the relative airspeed (deg)

All angles are positive for clockwise rotation. The angle from the relative airspeed vector to the chordline of the airfoil is the *angle of attack*, AOA , which is calculated as follows:

$$\begin{aligned}\alpha &= \theta - \varphi \\ \theta &= \gamma + \delta\end{aligned}\tag{A3}$$

where

α	angle of attack; angle from the relative airspeed to the airfoil chordline (deg)
θ	chord angle; angle from the direction of airfoil motion to chordline (deg)
γ	section built-in twist angle, positive for downstream twist of trailing edge (deg)
δ	blade pitch angle, positive for downstream pitch of trailing edge (deg)

Positive chord, twist, and pitch angles all rotate the trailing edge of a fan airfoil downstream and a wind turbine airfoil downwind.

In figure 1, the forces exerted on the airfoil section by the air stream are shown as acting in the plane of the section at a point that is 25 percent of the chord length from the leading edge, which is called the *quarter-chord point*. This point is often selected as the location where the longitudinal (lengthwise) axis of the blade, called the *stacking line*, intersects the plane of the airfoil section. In a fan blade, the stacking line is usually tilted upstream from a purely radial position at a small angle called the *coning* or *rake angle*, in order to balance steady axial airloads, which tend to bend the fan blade upstream, with steady centrifugal loads, which tend to bend a coned blade downstream. Similarly, the stacking line of a fan blade may be tilted away from the direction of motion by a small *sweepback angle*, in order to balance tangential airloads with centrifugal loads. In a wind turbine blade, the stacking line is often coned downwind and raked forward, again to balance steady aerodynamic loads with centrifugal loads.

In addition to the force components shown in figure 1, airloads can cause *pitching moment* loads about an axis through the quarter-chord point. Because the torsional stiffness of a fan or wind turbine blade is normally relatively high, pitching moments at the quarter-chord points in these airfoils can be assumed to be zero, or at least to have no significant effect on blade deflections or stresses. Pitching moments do affect the aerodynamic behavior of helicopter rotors, so the analysis of aerodynamic loads on torsionally-flexible helicopter blades or on blades with flexibility in their pitch-change mechanisms are beyond the scope of this study. Similarly, unsteady aerodynamic phenomena are not included here.

Airloads on a section of an airfoil are proportional to the *dynamic pressure* at that section, defined as follows:

$$pd = 0.5 \rho V_r^2\tag{A4}$$

where

pd	dynamic pressure (lb/ft ²)
ρ	air density (slugs/ft ³)

The *lift*, *drag*, and *resultant forces* acting on the section are defined as follows:

$$\begin{aligned} L &= CL \rho d c \\ D &= CD \rho d c \end{aligned} \tag{A5}$$

where

L lift force per unit span; force perpendicular to relative airspeed (lb/ft)
 CL lift coefficient; function of angle of attack, α
 c chord length (ft)
 D drag force per unit span; force in direction of relative airspeed (lb/ft)
 CD drag coefficient; function of angle of attack, α

The force components needed to calculate the action of the airflow on the rotor axis (for a turbine) or vice-versa (for a fan) are axial and tangential, relative to the axis, and these are calculated from the lift and drag components as follows:

$$\begin{aligned} F_x &= L \cos(\varphi) - D \sin(\varphi) \\ F_y &= L \sin(\varphi) + D \cos(\varphi) \\ F_r &= \sqrt{L^2 + D^2} = \sqrt{F_x^2 + F_y^2} \end{aligned} \tag{A6}$$

where

F_x axial force of air on airfoil per unit span; positive upstream (lb/ft)
 F_y tangential force of air on airfoil per unit span; positive opposite to motion (lb/ft)
 F_r resultant force of the air on the airfoil per unit span (lb/ft)

Appendix B—Contours of Airfoil Sections in Application Examples

Normalized coordinates of the NREL S809 [Tangler 2007] and Clark-Y airfoils are listed in tables B.1 and B.2. Chordwise dimensions, x , and thickness dimensions, y , are normalized by the chord width, c . Figures B.1 and B.2 show the section contours.

TABLE B.1—COORDINATES OF NREL S809 AIRFOIL

Upper Surface		Lower Surface	
x/c	y/c	x/c	y/c
0.00037	0.00275	0.00140	-0.00498
0.00575	0.01166	0.00933	-0.01272
0.01626	0.02133	0.02321	-0.02162
0.03158	0.03136	0.04223	-0.03144
0.05147	0.04143	0.06579	-0.04199
0.07568	0.05132	0.09325	-0.05301
0.10390	0.06082	0.12397	-0.06408
0.13580	0.06972	0.15752	-0.07467
0.17103	0.07786	0.19362	-0.08447
0.20920	0.08505	0.23175	-0.09327
0.24987	0.09113	0.27129	-0.10060
0.29259	0.09594	0.31188	-0.10589
0.33689	0.09933	0.35328	-0.10866
0.38223	0.10109	0.39541	-0.10842
0.42809	0.10101	0.43832	-0.10484
0.47384	0.09843	0.48234	-0.09756
0.52005	0.09237	0.52837	-0.08697
0.56801	0.08356	0.57663	-0.07442
0.61747	0.07379	0.62649	-0.06112
0.66718	0.06403	0.67710	-0.04792
0.71606	0.05462	0.72752	-0.03558
0.76314	0.04578	0.77668	-0.02466
0.80756	0.03761	0.82348	-0.01559
0.84854	0.03017	0.86677	-0.00859
0.88537	0.02335	0.90545	-0.00370
0.91763	0.01694	0.93852	-0.00075
0.94523	0.01101	0.96509	0.00054
0.96799	0.00600	0.98446	0.00065
0.98528	0.00245	0.99612	0.00024

TABLE B.2—COORDINATES OF CLARK-Y AIRFOIL

Upper Surface		Lower Surface	
x/c	y/c	x/c	y/c
0.000	0.000	0.000	0.000
0.005	0.027	0.005	-0.012
0.008	0.031	0.008	-0.016
0.013	0.038	0.013	-0.021
0.025	0.050	0.025	-0.030
0.050	0.068	0.050	-0.041
0.075	0.081	0.075	-0.047
0.100	0.091	0.100	-0.051
0.150	0.107	0.150	-0.055
0.200	0.117	0.200	-0.056
0.250	0.124	0.250	-0.055
0.300	0.128	0.300	-0.053
0.350	0.129	0.350	-0.050
0.400	0.127	0.400	-0.047
0.450	0.124	0.450	-0.044
0.500	0.118	0.500	-0.040
0.550	0.112	0.550	-0.037
0.600	0.104	0.600	-0.033
0.650	0.096	0.650	-0.029
0.700	0.086	0.700	-0.025
0.750	0.075	0.750	-0.021
0.800	0.062	0.800	-0.017
0.850	0.049	0.850	-0.013
0.900	0.035	0.900	-0.009
0.950	0.019	0.950	-0.006
1.000	0.002	1.000	-0.002
0.000	0.000	0.000	0.000
0.005	0.027	0.005	-0.012

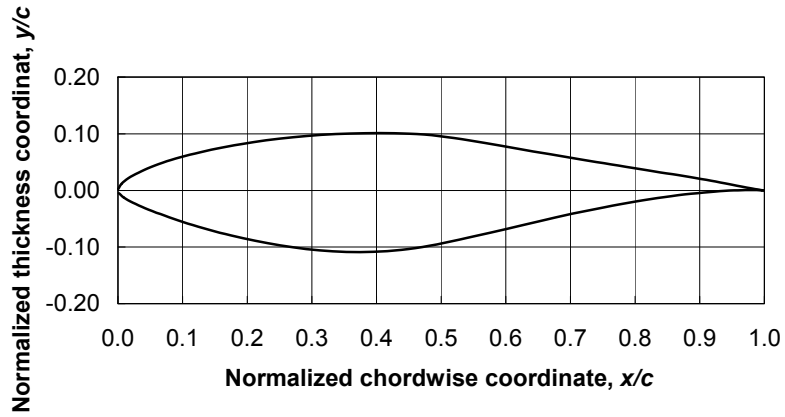


Figure B.1.—Contours of the NREL S809 airfoil section.

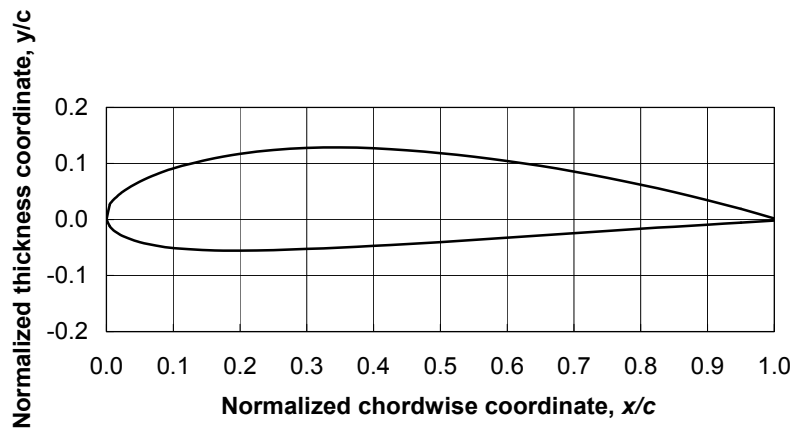


Figure B.2.—Contours of the Clark-Y airfoil section.

References

- Critzos, C.C., Heyson, H.H., and Boswinkle, R.W., Jr., 1955, "Aerodynamic Characteristics of NACA 0012 Airfoil Section at Angles of Attack from 0° to 180°," NACA TN 3361, National Advisory Committee for Aeronautics, Langley Aeronautical Laboratory.
- Gerber, B.S., Tangler, J.L., Duque, E.P.N., and Kocurek, J.D., 2005, "Peak and Post-Peak Power Aerodynamics from Phase VI NASA Ames Wind Turbine Data," *J. Solar Energy Engineering*, vol. 127, issue 2, May 2005, pp. 192–199.
- Hoerner, S.F., 1965, *Fluid-Dynamic Drag*, Hoerner Fluid Dynamics, Albuquerque, NM.
- Irvine, T.B., Kevdzija, S.S., Sheldon, D. W., and Spera, D. A., 2001, "Overview of the Icing and Flow Quality Improvements Program for the NASA-Glenn Icing Research Tunnel," AIAA-2001-0229, Cleveland, OH.
- Jacobs, E.N., and Anderson, R.F., 1929, "Characteristics of Airfoils as Tested in the Variable Density Wind Tunnel," NACA TR-352, National Advisory Committee for Aeronautics, Langley Aeronautical Laboratory.
- Lindenburg, C., 2000, "Stall Coefficients," ECN-RX-01-004, Energy Research Centre of the Netherlands, paper presented at IEA Symposium on the Aerodynamics of Wind Turbines, National Renewable Energy Laboratory.
- Lindenburg, C., 2003, "Investigation into Rotor Blade Aerodynamics," Netherlands Society for Energy and the Environment, Paper ECN-C-03-025.
- Ostowari, C., and Naik, D., "Post Stall Studies of Untwisted Varying Aspect Ratio Blades with an NACA 4415 Airfoil Section—Part I," *Wind Engineering*, vol. 8, no. 3, 1984, pp. 176–194.
- Somers, D.M., 1989, "Design and Experimental Results for the S809 Airfoil," Airfoils, Inc., State College, PA.
- Spera, D.A., 1995, "Bibliography of NASA-Related Publications on Wind Turbine Technology 1973-1995," DOE/NASA/5776-3, NASA CR-195462, NASA Lewis Research Center.
- Silverstein, A., 1934, "Scale Effect on Clark Y Airfoil Characteristics from N.A.C.A. Full-Scale Wind Tunnel Tests," NACA TR-502, National Advisory Committee for Aeronautics, Langley Aeronautical Laboratory.
- Sheldon, D. W., et al., 1996, "Results of Qualification Testing of Modifications to the NASA-Glenn Icing Research Tunnel," (unpublished).
- Tangler, J.L., and D.M. Somers, 1985, "Advanced Airfoils for HAWTS," *Proceedings, Wind Power '85 Conference*, SERI/CP-217-2902, Washington, DC: American Wind Energy Association, pp. 45–51.
- Tangler, J.L., 1987, "Status of Special-Purpose Airfoil Families," SERI/TP-217-3264, Golden, CO: National Renewable Energy Laboratory.
- Tangler, J.L., 2007, private communication.
- Tangler, J.L., and Ostowari, C., 1995, "Horizontal Axis Wind Turbine Post Stall Airfoil Characterization Synthesization," *Collected Papers on Wind Turbine Technology*, D.A. Spera, ed., DOE/NASA/5776-2, NASA CR-195432, pp. 35-39.
- Tangler, J., and Kocurek, J. David, 2004, "Wind Turbine Post-Stall Airfoil Performance Characteristics Guidelines for Blade-Element Momentum Methods," NREL/CP-500-36900, National Renewable Energy Laboratory.
- TU Delft, 2004, Wind Tunnel Test Data, as reported by Tangler and Kocurek, 2004.
- Viterna, L.A., 1982, "Theoretical and Experimental Power from Large Horizontal-Axis Wind Turbines," NASA TM-82944, NASA Lewis Research Center.
- Viterna, L.A., 1991, "Calculated Performance of the NASA Lewis Icing Research Tunnel," NASA TM-105173, NASA Lewis Research Center.

REPORT DOCUMENTATION PAGE			Form Approved OMB No. 0704-0188		
<p>The public reporting burden for this collection of information is estimated to average 1 hour per response, including the time for reviewing instructions, searching existing data sources, gathering and maintaining the data needed, and completing and reviewing the collection of information. Send comments regarding this burden estimate or any other aspect of this collection of information, including suggestions for reducing this burden, to Department of Defense, Washington Headquarters Services, Directorate for Information Operations and Reports (0704-0188), 1215 Jefferson Davis Highway, Suite 1204, Arlington, VA 22202-4302. Respondents should be aware that notwithstanding any other provision of law, no person shall be subject to any penalty for failing to comply with a collection of information if it does not display a currently valid OMB control number.</p> <p>PLEASE DO NOT RETURN YOUR FORM TO THE ABOVE ADDRESS.</p>					
1. REPORT DATE (DD-MM-YYYY) 01-10-2008		2. REPORT TYPE Final Contractor Report		3. DATES COVERED (From - To)	
4. TITLE AND SUBTITLE Models of Lift and Drag Coefficients of Stalled and Unstalled Airfoils in Wind Tunnels and Wind Turbines			5a. CONTRACT NUMBER NNC05CA95C		
			5b. GRANT NUMBER		
			5c. PROGRAM ELEMENT NUMBER		
6. AUTHOR(S) Spera, David, A.			5d. PROJECT NUMBER		
			5e. TASK NUMBER		
			5f. WORK UNIT NUMBER WBS 122711.03.07.03.02		
7. PERFORMING ORGANIZATION NAME(S) AND ADDRESS(ES) Jacobs Technology, Inc. Cleveland, Ohio 44135			8. PERFORMING ORGANIZATION REPORT NUMBER E-16599		
9. SPONSORING/MONITORING AGENCY NAME(S) AND ADDRESS(ES) National Aeronautics and Space Administration Washington, DC 20546-0001			10. SPONSORING/MONITOR'S ACRONYM(S) NASA		
			11. SPONSORING/MONITORING REPORT NUMBER NASA/CR-2008-215434		
12. DISTRIBUTION/AVAILABILITY STATEMENT Unclassified-Unlimited Subject Categories: 02 and 44 Available electronically at http://gltrs.grc.nasa.gov This publication is available from the NASA Center for AeroSpace Information, 301-621-0390					
13. SUPPLEMENTARY NOTES An errata was added to this document, June 2010.					
14. ABSTRACT Equations are developed with which to calculate lift and drag coefficients along the spans of torsionally-stiff rotating airfoils of the type used in wind turbine rotors and wind tunnel fans, at angles of attack in both the unstalled and stalled aerodynamic regimes. Explicit adjustments are made for the effects of aspect ratio (length to chord width) and airfoil thickness ratio. Calculated lift and drag parameters are compared to measured parameters for 55 airfoil data sets including 585 test points. Mean deviation was found to be -0.4 percent and standard deviation was 4.8 percent. When the proposed equations were applied to the calculation of power from a stall-controlled wind turbine tested in a NASA wind tunnel, mean deviation from 54 data points was -1.3 percent and standard deviation was 4.0 percent. Pressure-rise calculations for a large wind tunnel fan deviated by 2.7 percent (mean) and 4.4 percent (standard). The assumption that a single set of lift and drag coefficient equations can represent the stalled aerodynamic behavior of a wide variety of airfoils was found to be satisfactory.					
15. SUBJECT TERMS Aerodynamics lift; Aerodynamics drag; Stall; Wind turbine; Fan; Aero coefficient model; Wind tunnel					
16. SECURITY CLASSIFICATION OF:			17. LIMITATION OF ABSTRACT	18. NUMBER OF PAGES 38	19a. NAME OF RESPONSIBLE PERSON STI Help Desk (email:help@sti.nasa.gov)
a. REPORT U	b. ABSTRACT U	c. THIS PAGE U			19b. TELEPHONE NUMBER (include area code) 301-621-0390

